ACS Infectious Diseases

Article

pubs.acs.org/journal/aidcbc

Reduction of Influenza Virus Envelope's Fusogenicity by Viral Fusion Inhibitors

Michael Rowse,[†] Shihong Qiu,[†] Jun Tsao,[†] Yohei Yamauchi,[‡] Guoxin Wang,[§] and Ming Luo*[,§,∥]

[†]Department of Microbiology, University of Alabama at Birmingham, 1025 18th Street South, Birmingham, Alabama 35294, United States

[‡]Institute of Biochemistry, ETH Zurich, HPM E8.2, Otto-Stern-Weg 3, 8093 Zurich, Switzerland

[§]Laboratory of Structural Biology, School of Chemical Biology and Biotechnology, Peking University Shenzhen Graduate School, Shenzhen 518055, China

[∥]Department of Chemistry College of Arts and Sciences, Georgia State University, Atlanta, Georgia 30302, United States

Supporting Information

ABSTRACT: During cell entry of an enveloped virus, the viral membrane must be fused with the cellular membrane. The virus envelope has a unique structure consisting of viral proteins and a virus-specific lipid composition, whereas the host membrane has its own structure with host membrane proteins. Compound **136** was previously found to bind in close proximity to the viral envelope and inhibit influenza virus entry. We showed here that the **136**-treated influenza virus still caused hemolysis. When liposomes were used as the target membrane for **136**-treated viruses, aberrant fusion occurred; few liposomes fused per virion, and glycoproteins were not distributed evenly across fusion complexes. Additionally, large fusion aggregates did not form, and in some instances, neck-like structures were found. Based on previous results and hemolysis, fusion inhibition by **136** occurs post-scission but prior to lipid mixing.

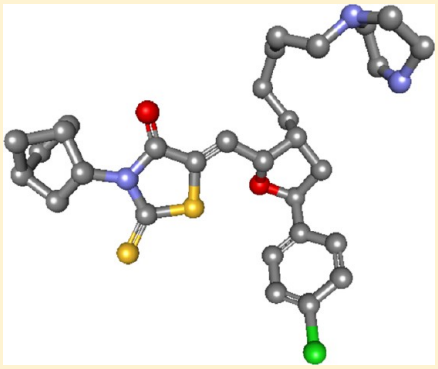

KEYWORDS: *lipid composition, liposome, fusogenicity, influenza virus, fusion inhibitor*

Membrane fusion is involved in a large number of biological processes in which contents are brought across the membrane. Membrane fusion is highly regulated by specific proteins. In addition, lipid composition is also a determining factor for membrane fusion. For infection by enveloped viruses, the membrane fusion step during virus entry must ensure that the virus genome is uncircuitously delivered to the right location within the host cell. For instance, the entry pathway of the influenza virus, a negative strand RNA virus that replicates in the nucleus, was followed by live imaging.[1] Binding of the viral host receptor recognition protein is the first step in the entry process. The attached virus particle is internalized in an endosome and trafficked to a location near the nucleus. There are three stages in the transport process. In the first stage, the virus-bearing endosome moves on the actin filaments, followed by dynein-directed translocation to the perinuclear region in the second stage. The third stage is an intermittent movement involving microtubule-based motilities in the perinuclear region, where acidification of the endosomal interior occurs. Membrane fusion takes place in a short time frame at the end of the trafficking. Along the pathway, host proteins that interact with the virus-bearing endosomes, such as Rab5/Rab7 and SNAREs, are recruited to the endosome. Rab5 regulates the functions of early endosomes, and Rab7 regulates the functions of late endosomes on which the entry of the influenza virus is dependent.[2] Before fusion takes place, SNARE complexes must be assembled on the endosomes.[3] A UV-radiation resistance-associated gene (UNRAG), an autophagic tumor suppressor, has been shown to be involved in the assembly of the SNARE complexes to promote viral fusion with the later endosomes.[4] It is clear that the fusion of the viral envelope membrane with the endosomal membrane during entry is highly regulated by host proteins associated with the endosomal membrane. The endocytic virus can program the endosomes to recruit specific cognate SNARE proteins onto the target membrane.[4] This membrane fusion process is not between two lipid vesicles without regulatory proteins.

Changing the membrane structure is an effective way to inhibit viral fusion. The interferon-induced transmembrane proteins (IFITMs) have been shown to be membrane-associated proteins and restrict virus infection.[5−8] They assert their antiviral effects by changing the properties of the cellular membrane. IFITM3 was shown to be targeted to endosomes through its N-terminal region.[9,10] IFITM3 is a type II transmembrane protein with a N-terminal intramembrane domain (IM1) and a C-terminal transmembrane domain (TM2) flanking a conserved intracellular loop (CIL).[8] Overexpression of IFITM proteins increased the lipid order, making the membrane less fluidized, which could be reversed

Received: July 6, 2015
Published: October 15, 2015

DOI: 10.1021/acsinfecdis.5b00109
ACS Infect. Dis. 2016, 2, 47−53

by addition of oleic acid that generates negative spontaneous curvature.[7] IFITM proteins also promote accumulation of cholesterol in the late endosomes.[11] The exact step at which IFITM3 inhibits membrane fusion was recently shown to be the pore expansion by altering the cytoplasmic leaflet.[12] The accumulated data suggest that restriction of the fluidity of the cellular membrane by IFITM proteins is an effective mechanism to block viral membrane fusion with the endosomal membrane.

Small-molecule inhibitors have been shown to inhibit membrane fusion of influenza virus. A number of inhibitor compounds can block conformational changes of influenza virus hemagglutinin (HA), which is required for HA to induce viral membrane fusion.[13] However, these inhibitors are HA-subtype-specific. Some inhibitors worked on H1 (e.g., RO5464466), H1−H2 (e.g., BYM-27709, CL 61917, and Stachyflin), or H3 (e.g., TBHQ and 4c). Other fusion inhibitors directly bind in the envelope and block viral fusion with cellular membranes.[14,15] These compounds appear to change the structure of the lipid envelope.

A potent fusion inhibitor, (*Z*)-3-(bicyclo[2.2.1]heptan-2-yl)-5-((5-(4′-chlorophenyl)-3-(3-(piperazin-1-yl)pentyl)furan-2-yl)methylene)-2-thioxothiazolidin-4-one (named compound **136**), was shown to block fusion of the viral envelope with the cellular membrane.[16] In this study, we show that **136** reduces the fusogenicity of the influenza virus envelope. **136** appears to alter the structure of the viral membrane, so it could not fuse with the more rigid endosomal membrane, as shown by electron microscopic images of lipid−influenza virus fusion, in contrast to IFITM proteins that restrict the fluidity of the cellular membrane to block fusion.

RESULTS

Crystal Structure. In previous studies, a potent fusion inhibitor, compound **136**, was shown to inhibit influenza virus infection (X-31) with an EC_{50} value of 50 pM and a selectivity index of 1×10^6.[16] Because of the high potency and selectivity index of **136**, further in vitro characterization was carried out. The crystal structure of a compound (**7937**) that represents the main **136** body indicates that compound **136** has a rigid configuration and has a shape similar to that of cholesterol, except for the flexible linker (Figure 1 and Supporting Information Figure S1 and Table S1).

Hemolysis. In the fusion model proposed by Lee,[17] scission of the target membrane occurs prior to lipid mixing with the influenza virus. Red blood cells (RBCs) have been used to study fusion of the influenza virus with authentic plasma membranes. During the fusion process, the influenza virus breaks the RBC plasma membrane, allowing hemoglobin to leak into the bulk solution. The RBCs can be spun down, and the extent of hemoglobin leakage into the bulk solution can be quantitated by measuring the absorbance at 540 nm. Influenza virus treated with DMSO or the control compound **211** ((*E*)-*endo*/*exo*-1-(bicyclo[2.2.1]heptan-2-yl)-3-((5-(4-chlorophenyl)-3-(5-hydroxypentyl)furan-2-yl)methylene)pyrrolidine-2,5-dione) caused hemolysis at pH 5.6 or less, as anticipated (Figure 1E). Influenza virus treated with **136** also induced hemolysis but to a slightly greater extent at pH 5.2−5.8 (Figure 1D). The exact cause for this increase is not clear. We speculate that HA molecules in **136**-treated virions may be able to aggregate somewhat more to induce a slightly increased pore size. The same level of hemolysis is achieved at pH 5.0 with DMSO, **211**, and **136** treatment, indicating that scission of the host cell target membrane is not inhibited. Based on a previous study[16] that found that **136** blocks lipid mixing with authentic cellular membranes, we conclude that **136** inhibits viral fusion post-scission of the target membrane but prior to lipid mixing.

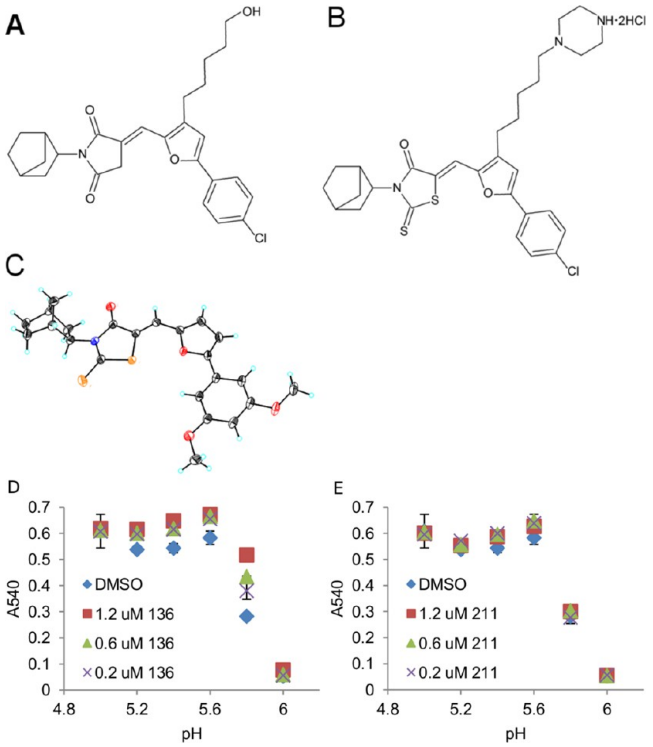

Figure 1. Structure of compounds **136** and **211**, crystal structure of a related compound, and hemolysis analysis. (A,B) Line drawings of the chemical structure of compounds **211** and **136**, respectively. (C) Crystal structure of compound **7937**, a compound analogous to **136**. Due to the flexible aliphatic chain of **136**, it was not successfully crystallized. (D) Hemolysis assays were conducted with **136** or (E) **211**-treated viruses. Because hemolysis requires concentrated virus, 0.2 μM is the EC_{50}, 0.6 μM is the EC_{90}, and 1.2 μM is the EC_{99} for **136**. **136** treatment at pH 5.8 caused significantly different hemolysis ($P < 0.01$) between all samples. Treatment with **136** caused significantly more hemolysis at pH 5.2−5.6 (one-way ANOVA, post-hoc Tukey test, $P < 0.05$) as compared to DMSO. Hemolysis was not affected by treatment with **211**. At pH 5.0, hemolysis is equivalent in all samples. Representative data show two independent experiments. Data points are the average of two replicates ± SD.

Electron Microscopy. To directly visualize how **136**-treated X-31 virus fused in vitro to liposomes, negative stained electron microscopy was performed. As a control, **136**-treated virus and liposomes were mixed at pH 7.5, as shown in Figure 2A. Clearly, the virus is intact and appears identical to the untreated, DMSO-treated, or **211**-treated virus (data not shown). Liposomes are visible, as well. The same samples were also acidified to pH 5.0 to initiate fusion of virus to liposomes. Most DMSO- or **211**-treated virions fused with liposomes, trapping unfused virions (Figure 2B), or fused extensively with many virions and liposomes (Figure 2C). The unfused viruses in these aggregates are not available to fuse with liposomes simply because of steric hindrance by the surrounding fused virus particles and liposomes. The portion of DMSO- and **211**-treated viruses that were not incorporated into aggregates fused to liposomes with an even distribution of virus glycoproteins in the liposome lipids. Figure 2I shows an example of evenly distributed viral glycoproteins in liposome

DOI: 10.1021/acsinfecdis.5b00109
ACS Infect. Dis. 2016, 2, 47−53

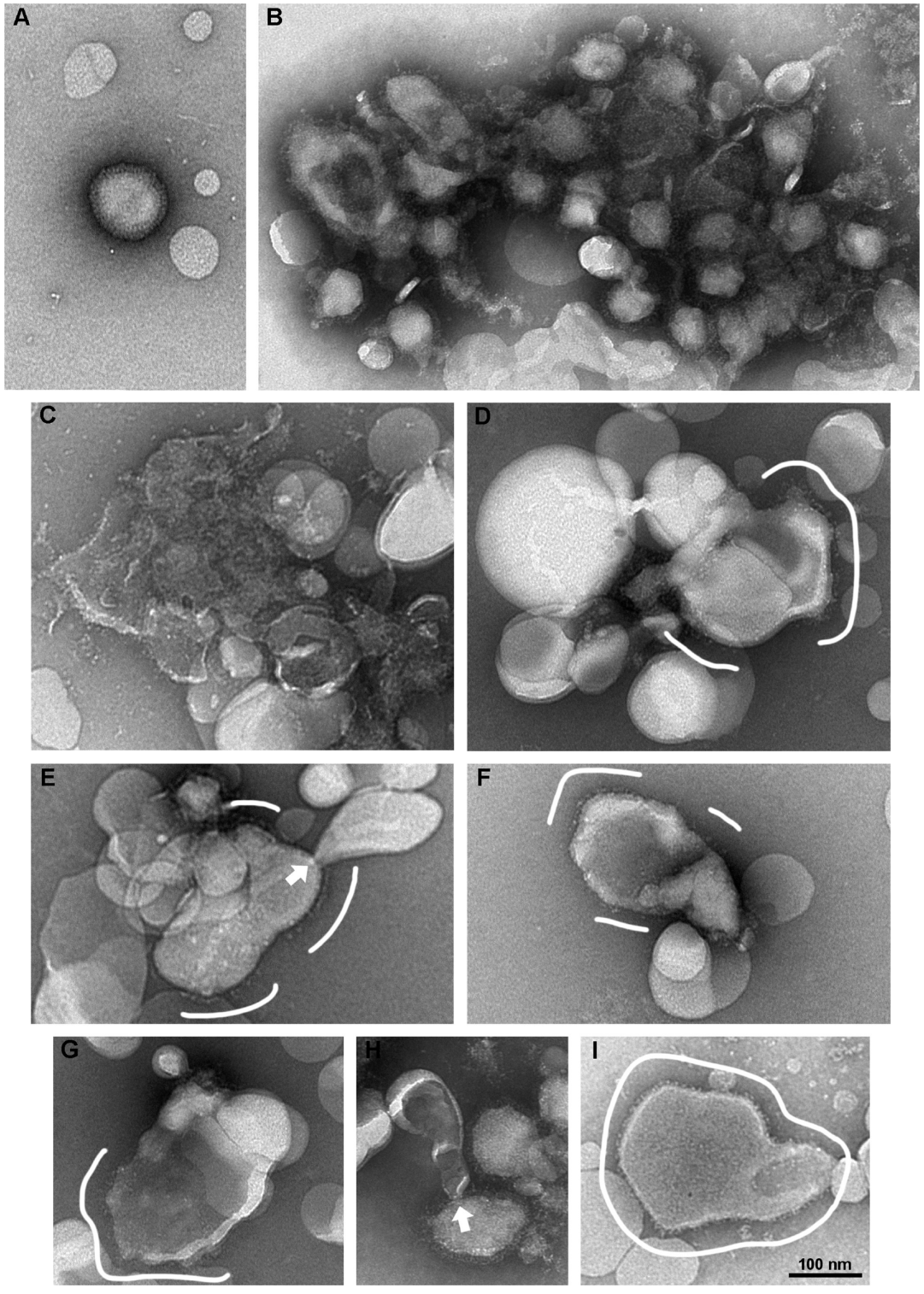

Figure 2. Fusion of the **136**-treated virus with liposomes results in less aggregation and uneven glycoprotein distribution. **136**-treated virions and liposomes at pH 7.5 (A). All other samples had the same concentrations of virions and liposomes and were acidified to pH 5.0. (B) Most **211**-treated virions fused with liposomes, trapping unfused virions, or (C) fused extensively with many virions and liposomes. **136**-treated virions fused to liposomes, but uneven glycoprotein distribution was observed. (D−G,I) White lines indicate continuous glycoprotein stretches on the surface of fused virions and liposomes. (E,H) Some **136**-treated virions form a neck-like structure that was not observed in the **211**-treated samples. The white arrows point to the neck structures. (I) Complete fusion with **211**-treated virions and liposomes shows even glycoprotein mixing. Scale bar: 100 nm.

lipids after fusion. Some virus particles treated with **136** were able to undergo fusion with liposomes, but the extent was greatly reduced (Figure 2D−G). Instead of one particle fusing with multiple liposomes in the case of the wild-type virus particles, fusion of the influenza virus treated with **136** usually occurred with just one liposome, and examples of large aggregates like those shown in Figure 2B,C were not found. In addition, these samples had an uneven distribution of viral

DOI: 10.1021/acsinfecdis.5b00109
ACS Infect. Dis. 2016, 2, 47−53

glycoproteins on the surface of the fused virus and liposome membrane, as shown in Figure 2D−G. The solid white lines indicate the regions where viral glycoproteins are present. Some **136**-treated viruses were found occasionally to form a neck-like structure (white arrows) by bringing a liposomal membrane into close proximity to the viral membrane but did not appear to induce lipid mixing (Figure 2E,H, white arrows). Similar situations were not observed in DMSO- or **211**-treated samples, although it is possible that such structures could be present in the large aggregates but are refractory to imaging. The neck-like structures between liposomes and **136**-treated virus in Figure 2E,H may reflect how scission of the target membrane could occur, but lipid mixing is blocked at cellular membranes.

Lipid Mixing. To gain further insight into how **136** blocks fusion to cellular membranes, we tested lipid mixing of the DiD-labeled X-31 virus with liposomes by lowering the pH and monitoring the dequenching of DiD for 20 min. Samples treated with DMSO or **211** dequenched similarly (Figure 3).

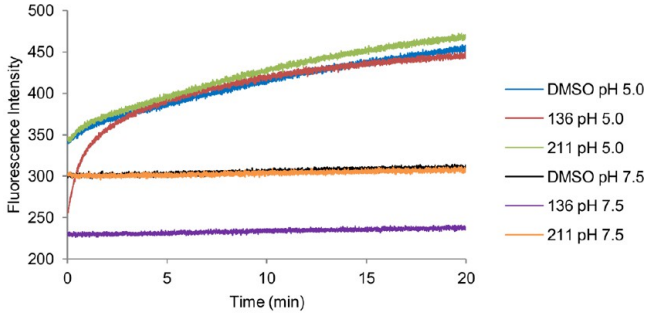

Figure 3. 136 quenches the DiD baseline fluorescence and affects the lipid mixing rate. DiD-labeled X-31 virus was fused to liposomes by lowering the pH. The reaction progress was monitored as an increase in fluorescence intensity due to dequenching of DiD as it mixes with liposome lipids. As a negative control, dequenching at pH 7.5 was measured. The baseline fluorescence at pH 7.5 is the same for DMSO- and **211**-treated samples, but the fluorescence signal is significantly quenched by **136**. The initial rate of dequenching was slowed by the **136** treatment of virions. Final dequenching was nearly identical for all pH 5.0 samples. A 5 point moving average was applied to all samples to smooth the data.

The initial lipid mixing took place faster than what could be measured by our instrument. Samples treated with **136** dequenched at a slower initial rate, but all the samples achieve the same extent of dequenching after 20 min. Importantly, **136** quenched the DiD baseline fluorescence to a further extent than when DMSO or **211** was used to treat viruses. The baseline at pH 7.5 with DMSO or **211** is about 305 fluorescence units, and with **136**, the baseline shifts to about 230 fluorescence units. The quenching of DiD at the baseline suggests that **136** binds to the virion in close proximity to DiD in the viral membrane.

Content Mixing. Based on the **136**-treated influenza virus mixing lipids with liposomes, we decided to quantitate content mixing in the liposome system using the same virus and liposome concentrations as shown in Figure 2. To accurately quantitate the extent of content mixing, we encapsulated the liposomes with trypsin and initiated the fusion reaction (Figure 4). If trypsin inside the liposomes was able to mix with the contents of the virus, then trypsin would degrade the M1 and NP proteins. If trypsin was to leak outside of the liposomes,

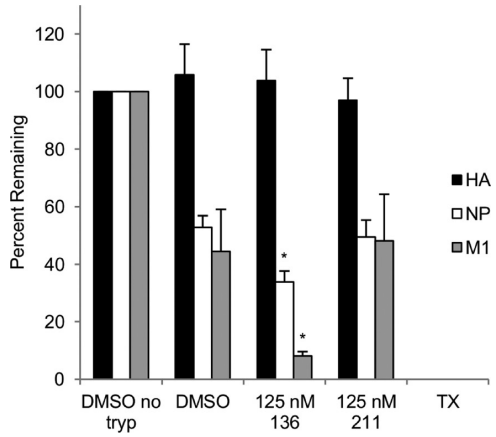

Figure 4. 136-treated virions mix contents with liposomes. Inhibitor-treated X-31 virus was fused to liposomes containing trypsin or empty liposomes as a control. The level of each protein was normalized to the control sample of the X-31 virus and liposomes without trypsin (DMSO no tryp). DMSO and 125 nM **211**-treated virions both showed that approximately 50% of NP and M1 were degraded by trypsin. The 125 nM **136**-treated virions (125 nM was used to make sure 99% virions were treated by **136**) showed apparently more degradation of NP and M1 by trypsin (one-way ANOVA, post-hoc Tukey test, $P < 0.01$). When Triton X-100 was added to **136**-treated samples, complete degradation of all proteins occurred (TX).

then it would degrade HA. Because trypsin is a 23 kDa protein, a large pore connecting the lumen of the liposome to the interior of the virus must be present if M1 and NP are degraded. We found that DMSO- and **211**-treated viruses allowed approximately one-half of the M1 and NP proteins to be degraded in the sample. We believe that the aggregation caused by extensive fusion between the liposomes and virus prevented further degradation of the M1 and NP proteins. Interestingly, with the **136**-treated virus, we saw an increase (one-way ANOVA, post-hoc Tukey test, $P < 0.01$) in trypsin digestion of M1 and NP but not of HA as compared to DMSO- and **211**-treated samples. A virus treated with **136** can undergo more content mixing during fusion to liposomes due to less aggregation in comparison with DMSO- and **211**-treated viruses, but fusion is arrested during fusion to cellular membranes. This suggests that the composition of the target membrane is a critical factor for inhibition by **136**. Aggregation trapping of unfused virions and liposomes explains why **211**- and DMSO-treated samples exhibited less content mixing (Figure 2C).

■ DISCUSSION

Fusion inhibition by small molecules is a promising mechanism to target with antiviral agents.[18] Compound **136** was previously shown by live imaging to be a potent inhibitor that prevents fusion of the influenza virus with the cellular membrane.[16] Trypsin digestion studies further revealed that the inhibitors do not destroy the viral envelope, destabilize hemagglutinin, or prevent the low pH-induced conformational change of HA.

The EM images of the X-31 virus with and without treatment with **136** revealed two different modes of membrane fusion with liposomes. The virus treated with DMSO or **211** was robust in fusion with liposomes. One virus particle was shown to fuse with multiple liposomes to form large aggregates (Figure 2B). On the other hand, the virus treated with **136** appeared to have lost its high fusion potential, even though

DOI: 10.1021/acsinfecdis.5b00109
ACS Infect. Dis. 2016, 2, 47−53

fusion with liposomes was not completely blocked. This observation is consistent with the result from our studies on **136**-treated viruses with cellular membranes in which fusion was reduced to 20% of untreated viruses.[16] The **136**-treated virus could not fuse with many liposomes to form large fusion aggregates like the **211**-treated virus. In cases where aberrant fusion occurred, the glycoproteins were not distributed across the whole membrane (Figure 2D−G). Sometimes the **136**-treated virus fusion could not proceed to completion (Figure 2E,H). This may reflect how the fusion process was arrested when authentic cellular membranes were used as target membranes.[16]

In vitro studies of the **136**-treated influenza virus suggest that the structure of the viral envelope was changed by binding of **136** to the virion. The baseline fluorescence of DiD-labeled virions was further reduced by treatment with **136** but not **211** or DMSO, suggesting that **136** binds in close proximity to the membrane-bound DiD (Figure 3). Lipid mixing of DMSO-, **136**-, or **211**-treated DiD-labeled virus with liposomes occurred to the same extent, although the initial rate of lipid mixing was slower in **136**-treated samples (Figure 3). This observation can be explained by the pattern of the **136**-treated virus with liposomes. Since no aggregates or trapped virions were present, the lipid mixing could be initiated simultaneously between a large number of virions and liposomes. The initiation of lipid mixing occurred more slowly at the beginning due to inhibition by **136**, but eventually, lipid mixing reached the same extent as the **211**-treated virus. The content exchange between the **136**-treated virus and liposomes with encapsulated trypsin was also more complete because of the same reason (Figure 4).

During enveloped virus assembly, the virus buds at the host cell membrane. For viruses, such as influenza virus, the viral glycoproteins and other envelope proteins are concentrated at membrane microdomains.[19] In the released virus progenies, the virus envelope has a lipid composition rich in sphingolipids and cholesterol, which is very different from the cellular membrane.[20] It has been shown that the cholesterol content in the membrane has various effects on the fusion kinetics of enveloped viruses.[21] It is also shown that the transmembrane domains of viral glycoproteins play an important role in the fusogenicity of the viral envelope.[22] The unique structure of the viral envelope is constructed with virus-specific lipid composition and the transmembrane domains of viral glycoproteins.[23] Fusion inhibitors, like compound **136**, may bind in the viral envelope, reduce fusogenicity of the virus, and block fusion post-scission but prior to lipid mixing with cellular membranes.

From previous studies, we found that **136** blocks lipid mixing of the influenza virus with the endosomal membrane of human lung epithelial cells.[16] Additionally, when **136**-treated influenza virus was fused at the plasma membrane of human lung epithelial cells analogous to the liposome assays performed in this work, lipid mixing was blocked.[16] Here we have narrowed down the step of the fusion pathway blocked by **136** to post-scission of the host cell membrane and prior to lipid mixing. In vitro liposome fusion assays revealed that **136**-treated viruses lost their high fusion potential and exhibited aberrant fusion to liposomes with limited distribution of viral glycoproteins. In some instances, the **136**-treated virions did not complete fusion; instead, a neck-like structure between the viral membrane and the liposomal membrane was present. This may reflect how fusion is arrested by **136** at the plasma membrane and endosomal membranes of human lung epithelial cells.

METHODS

Crystallization. A vial in a vial technique was used to crystallize compound **7937**. The inner vial contained 0.5 mL of 25 mg/mL **7937** dissolved in chloroform. The outer vial contained 4.5 mL of pentane. The outer vial was sealed and left at room temperature for 1 week. Large single crystals appeared in the inner vial within 1 week. Crystals were shipped to the X-ray Crystallography Center at Emory University for structure determination.

Cells and Viruses. MDCK-2 cells were cultured in Eagle's minimum essential medium supplemented with 5% fetal bovine serum and penicillin/streptomycin. All influenza viruses were grown in MDCK-2 cells. Influenza virus strain X-31 (H3N2) was amplified by infecting confluent MDCK-2 cells at an MOI of 0.001. Viruses were purified on a 20−50% sucrose gradient by centrifugation for 1.75 h at 60 000 rcf.

Preparation of Liposomes and Fluorescently Labeled Virus. Similar to the method described by Schmidt et al.,[24] POPC, POPE, and cholesterol were dissolved in chloroform/methanol (2:1) to make stock solutions. Liposomes composed of POPC/POPE/cholesterol (1:1:2) were made by mixing aliquots of the POPC, POPE, and cholesterol stock solutions in a glass vial. The solvent was evaporated with a stream of nitrogen, leaving a thin film of lipids on the bottom of the glass vial. Residual solvent was removed by leaving the samples under high vacuum (less than 10 μm mercury) overnight. To produce 100 nm unilamellar liposomes, samples were hydrated at 2 mg/mL in 10 mM HEPES, 100 mM NaCl, pH 7.5. The hydrated liposomes were subject to five cycles of freeze-and-thaw using liquid nitrogen and a 37 °C water bath, then extruded through a 100 nm diameter polycarbonate filter 21 times (Avanti Polar Lipids). X-31 virus was labeled with DiD by directly adding a 5 μL aliquot of DiD Vybrant solution to 500 μL of 2 mg/mL virus sample. Labeling was performed for 2 h at 37 °C with constant shaking. Unincorporated dye was removed by centrifugation at 60 000 rcf for 30 min, and the pellet was resuspended in 10 mM HEPES, 100 mM NaCl, pH 7.5.

Fusion Assays with Liposomes and Fluorescently Labeled Virus. X-31 virus was preincubated for 20 min with various concentrations of **136**, **211**, or DMSO only. Liposomes were added to the sample to a final concentration of 40 μg/mL X-31 virus and 1.5 mg/mL liposomes. To initiate fusion, the pH of the mixture was reduced to 5.0 using an aliquot of 10 mM HEPES, 100 mM NaCl, 50 mM citrate, pH 3.0. Fusion progress was monitored by fluorescence measurements of DiD at λ_{EX} = 644 nm/λ_{EM} = 665 nm. All fluorescence measurements were performed with continuous data collection for 20 min using a Cary Eclipse spectrofluorometer (Varian). The intensity of fluorescence was normalized by adding aliquots of Triton X-100 to each cuvette and recording the maximal fluorescence measurements. The formula for normalizing fluorescence measurements was $[F(t) - F(0)]/[F_{TX\text{-}100} - F(0)]$, where $F(t)$ is the fluorescence intensity at a time point, $F(0)$ is the initial fluorescence measurement, and $F_{TX\text{-}100}$ is the maximal fluorescence measurement after adding Triton X-100.

Hemolysis Assay. One microliter aliquots of inhibitor stocks were added to the wells of a 96-well plate. As a control, 1 μL of DMSO only was added to the wells. Next, 100 μL of X-31 virus at 10^8 pfu/mL was added to the wells and mixed. Then, 100 μL of chicken red blood cells in DPBS was added to

DOI: 10.1021/acsinfecdis.5b00109
ACS Infect. Dis. 2016, 2, 47−53

each well at a final concentration of 1% and incubated at 37 °C for 10 min. The plate was subjected to centrifugation at 3000 rpm for 2 min, and the supernatant was removed. To initiate hemolysis, 250 μL of 138 mM NaCl/10 mM citrate, pH 5.0−6.0, was added to the appropriate wells. To establish the baseline level of hemolysis, 138 mM NaCl/10 mM HEPES, pH 7.5, was added to a well. The plate was placed in an incubator at 37 °C for 10 min. Cells were pelleted at 3000 rpm, and 200 μL of supernatant was transferred to a new 96-well plate. OD_{540} was measured using a Biotek Synergy HT plate reader.

Negative Stain Electron Microscopy. Equal volumes of 10 μg/mL X-31 virus and 250 μg/mL liposomes were mixed, acidified with an aliquot of 50 mM citrate, pH 3.0, and incubated for 20 min at 37 °C. Samples were reneutralized with an aliquot of 100 mM Tris, pH 10.0, and incubated at 37 °C for 1 h. Seven microliters of sample was applied to a glow-discharged carbon-coated grid for 30 s, blotted with filter paper, stained with 7 μL of 1% phosphotungstic acid, pH 7.5, for 20 s, and blotted again. Samples were imaged with a FEI Tecnai 12 transmission electron microscope.

Trypsin Mixing Assay. Liposomes were prepared as above, except 10 mg/mL trypsin was included during hydration and freeze-thawing was omitted to preserve enzymatic activity. Excess trypsin that was not encapsulated into liposomes was removed by dialysis, and trace amounts of trypsin were removed by passing the liposomes over a 2 mL STI-agarose conjugated column (GE healthcare) according to the manufacturer's instructions. Equal volumes of 10 μg/mL X-31 virus and 250 μg/mL liposomes were mixed, acidified with an aliquot of 50 mM citrate, pH 3.0, and incubated for 20 min at 37 °C. Samples were reneutralized with an aliquot of 100 mM Tris, pH 10.0, and incubated at 37 °C for 1 h. The reaction was terminated by addition of 2 mM AEBSF for 20 min at 37 °C. The samples were electrophoresed on a 10% nonreducing polyacrylamide gel. Gels were stained with SYPRO ruby and imaged with a CCD-based gel imager (Syngene G:box). ImageJ was used for quantitation of protein bands.

■ ASSOCIATED CONTENT

Supporting Information

The Supporting Information is available free of charge on the ACS Publications website at DOI: 10.1021/acsinfecdis.5b00109.

X-ray crystallographic information for compound **7937** (PDF)

■ AUTHOR INFORMATION

Corresponding Author

*Telephone: 404-413-6608. Fax: 404-413-5500. E-mail: mluo@gsu.edu.

Author Contributions

All authors contributed to experiments. M.R., Y.Y., G.X.W., and M.L. wrote the article.

Notes

The authors declare the following competing financial interest(s): The compounds have been included in a patent in which Guoxin Wang and Ming Luo are inventors.

■ ACKNOWLEDGMENTS

This work is supported in part by NIH grants (AI-080699 and U54-AI-057157) and a grant from Shenzhen Municipal Government (ZDSY20130331145112855) to M.L.

■ ABBREVIATIONS

AEBSF, 4-(2-aminoethyl)benzenesulfonyl fluoride; CIL, conserved intracellular loop; DiD, 1,10-dioctadecyl-3,3,30,30-tetramethylindodicarbocyanine perchlorate; HA, hemagglutinin; IFITM, interferon-induced transmembrane protein; IM1, intramembrane domain 1; M1, matrix protein; MDCK, Madin-Darby canine kidney; NP, nucleoprotein; POPC, 1-palmitoyl-2-oleoyl-*sn*-glycero-3-phosphocholine; POPE, 1-palmitoyl-2-oleoyl-*sn*-glycero-3-phosphoethanolamine; RBC, red blood cell; SNARE, soluble *N*-ethylmaleimide-sensitive factor activating protein receptor; STI, soybean trypsin inhibitor; TM, transmembrane; UNRAG, UV-radiation resistance-associated gene

■ REFERENCES

(1) Lakadamyali, M., Rust, M. J., Babcock, H. P., and Zhuang, X. (2003) Visualizing infection of individual influenza viruses. *Proc. Natl. Acad. Sci. U. S. A. 100*, 9280−9285.

(2) Sieczkarski, S. B., and Whittaker, G. R. (2003) Differential requirements of Rab5 and Rab7 for endocytosis of influenza and other enveloped viruses. *Traffic 4*, 333−343.

(3) Jahn, R., and Scheller, R. H. (2006) SNAREs–engines for membrane fusion. *Nat. Rev. Mol. Cell Biol. 7*, 631−643.

(4) Pirooz, S. D., He, S., Zhang, T., Zhang, X., Zhao, Z., Oh, S., O'Connell, D., Khalilzadeh, P., Amini-Bavil-Olyaee, S., Farzan, M., and Liang, C. (2014) UVRAG is required for virus entry through combinatorial interaction with the class C-Vps complex and SNAREs. *Proc. Natl. Acad. Sci. U. S. A. 111*, 2716−2721.

(5) Brass, A. L., Huang, I. C., Benita, Y., John, S. P., Krishnan, M. N., Feeley, E. M., Ryan, B. J., Weyer, J. L., van der Weyden, L., Fikrig, E., Adams, D. J., Xavier, R. J., Farzan, M., and Elledge, S. J. (2009) The IFITM proteins mediate cellular resistance to influenza A H1N1 virus, West Nile virus, and dengue virus. *Cell 139*, 1243−1254.

(6) Everitt, A. R., Clare, S., Pertel, T., John, S. P., Wash, R. S., Smith, S. E., Chin, C. R., Feeley, E. M., Simms, J. S., Adams, D. J., Wise, H. M., Kane, L., Goulding, D., Digard, P., Anttila, V., Baillie, J. K., Walsh, T. S., Hume, D. A., Palotie, A., Xue, Y., Colonna, V., Tyler-Smith, C., Dunning, J., Gordon, S. B., Smyth, R. L., Openshaw, P. J., Dougan, G., Brass, A. L., and Kellam, P. (2012) IFITM3 restricts the morbidity and mortality associated with influenza. *Int. J. Infect. Dis. 16*, e79.

(7) Li, K., Markosyan, R. M., Zheng, Y. M., Golfetto, O., Bungart, B., Li, M., Ding, S., He, Y., Liang, C., Lee, J. C., Gratton, E., Cohen, F. S., and Liu, S. L. (2013) IFITM proteins restrict viral membrane hemifusion. *PLoS Pathog. 9*, e1003124.

(8) Bailey, C. C., Kondur, H. R., Huang, I. C., and Farzan, M. (2013) Interferon-induced transmembrane protein 3 is a type II transmembrane protein. *J. Biol. Chem. 288*, 32184−32193.

(9) Jia, R., Pan, Q., Ding, S., Rong, L., Liu, S. L., Geng, Y., Qiao, W., and Liang, C. (2012) The N-terminal region of IFITM3 modulates its antiviral activity by regulating IFITM3 cellular localization. *Journal of virology 86*, 13697−13707.

(10) Jia, R., Xu, F., Qian, J., Yao, Y., Miao, C., Zheng, Y. M., Liu, S. L., Guo, F., Geng, Y., Qiao, W., and Liang, C. (2014) Identification of an endocytic signal essential for the antiviral action of IFITM3. *Cell. Microbiol. 16*, 1080−1093.

(11) Amini-Bavil-Olyaee, S., Choi, Y. J., Lee, J. H., Shi, M., Huang, I. C., Farzan, M., and Jung, J. U. (2013) The antiviral effector IFITM3 disrupts intracellular cholesterol homeostasis to block viral entry. *Cell Host Microbe 13*, 452−464.

(12) Desai, T. M., Marin, M., Chin, C. R., Savidis, G., Brass, A. L., and Melikyan, G. B. (2014) IFITM3 restricts influenza A virus entry by blocking the formation of fusion pores following virus-endosome hemifusion. *PLoS Pathog. 10*, e1004048.

(13) Vanderlinden, E., and Naesens, L. (2014) Emerging antiviral strategies to interfere with influenza virus entry. *Med. Res. Rev. 34*, 301−339.

(14) Wolf, M. C., Freiberg, A. N., Zhang, T., Akyol-Ataman, Z., Grock, A., Hong, P. W., Li, J., Watson, N. F., Fang, A. Q., Aguilar, H.

DOI: 10.1021/acsinfecdis.5b00109
ACS Infect. Dis. 2016, 2, 47−53

C., Porotto, M., Honko, A. N., Damoiseaux, R., Miller, J. P., Woodson, S. E., Chantasirivisal, S., Fontanes, V., Negrete, O. A., Krogstad, P., Dasgupta, A., Moscona, A., Hensley, L. E., Whelan, S. P., Faull, K. F., Holbrook, M. R., Jung, M. E., and Lee, B. (2010) A broad-spectrum antiviral targeting entry of enveloped viruses. *Proc. Natl. Acad. Sci. U. S. A. 107*, 3157−3162.

(15) Colpitts, C. C., Ustinov, A. V., Epand, R. F., Epand, R. M., Korshun, V. A., and Schang, L. M. (2013) 5-(Perylen-3-yl)ethynyl-arabino-uridine (aUY11), an arabino-based rigid amphipathic fusion inhibitor, targets virion envelope lipids to inhibit fusion of influenza virus, hepatitis C virus, and other enveloped viruses. *Journal of virology 87*, 3640−3654.

(16) Rowse, M., Qiu, S., Tsao, J., Xian, T., Khawaja, S., Yamauchi, Y., Yang, Z., Wang, G., and Luo, M. (2015) Characterization of potent fusion inhibitors of influenza virus. *PLoS One 10*, e0122536.

(17) Lee, K. K. (2010) Architecture of a nascent viral fusion pore. *EMBO J. 29*, 1299−1311.

(18) Berkhout, B., Eggink, D., and Sanders, R. W. (2012) Is there a future for antiviral fusion inhibitors? *Curr. Opin. Virol. 2*, 50−59.

(19) Lyles, D. S. (2013) Assembly and budding of negative-strand RNA viruses. *Adv. Virus Res. 85*, 57−90.

(20) Gerl, M. J., Sampaio, J. L., Urban, S., Kalvodova, L., Verbavatz, J. M., Binnington, B., Lindemann, D., Lingwood, C. A., Shevchenko, A., Schroeder, C., and Simons, K. (2012) Quantitative analysis of the lipidomes of the influenza virus envelope and MDCK cell apical membrane. *J. Cell Biol. 196*, 213−221.

(21) Domanska, M. K., Wrona, D., and Kasson, P. M. (2013) Multiphasic effects of cholesterol on influenza fusion kinetics reflect multiple mechanistic roles. *Biophys. J. 105*, 1383−1387.

(22) Kemble, G. W., Danieli, T., and White, J. M. (1994) Lipid-anchored influenza hemagglutinin promotes hemifusion, not complete fusion. *Cell 76*, 383−391.

(23) Victor, B. L., Baptista, A. M., and Soares, C. M. (2012) Structural determinants for the membrane insertion of the trans-membrane peptide of hemagglutinin from influenza virus. *J. Chem. Inf. Model. 52*, 3001−3012.

(24) Schmidt, A. G., Yang, P. L., and Harrison, S. C. (2010) Peptide inhibitors of dengue-virus entry target a late-stage fusion intermediate. *PLoS Pathog. 6*, e1000851.

DOI: 10.1021/acsinfecdis.5b00109
ACS Infect. Dis. 2016, 2, 47−53